PHILOSOPHICAL TRANSACTIONS OF THE ROYAL SOCIETY B BIOLOGICAL SCIENCES

Molecular Crystals and Liquid Crystals: New Results for t-Butyl Chloride

J. C. Frost, A. J. Leadbetter and R. M. Richardson

Phil. Trans. R. Soc. Lond. B 1980 **290**, 567-582
doi: 10.1098/rstb.1980.0116

Phil. Trans. R. Soc. Lond. B **290**, 567–582 (1980)
Printed in Great Britain

Molecular crystals and liquid crystals: new results for *t*-butyl chloride

By J. C. Frost[†][‡], A. J. Leadbetter[†] and R. M. Richardson[§]
[†] *Chemistry Department, University of Exeter, Exeter EX4 4QD, U.K.*
[§] *Rutherford Laboratory, Chilton, Didcot, Oxon. OX11 0QX, U.K.*

The main theme of this paper is the use of incoherent quasielastic scattering to study molecular reorientational motions in molecular and liquid crystals at temperatures where a classical description is appropriate. The relation to quantum mechanical tunnelling between orientational potential wells of hydrogenous species (e.g. CH_3, NH_4^+) is mentioned briefly.

The use of this technique is illustrated with a description of the determination of the nature and dynamics of the molecular reorientations in the solid phases of *t*-butyl chloride. This shows how the measurement of the quasielastic spectrum as a function of scattering vector permits an identification of the type of reorientation and its characteristic time scale, provided this is fast enough to be observed in a neutron experiment ($\tau \gtrsim 10^{-9}$ s).

Finally a brief résumé is given of the results that have emerged from such studies about the various molecular motions that characterize and distinguish different liquid crystal phases.

1. Introduction

Very many substances have one or more phases in which the molecules are orientationally disordered. This disorder must in general be dynamic and is important in determining the properties of the phase. Furthermore, the understanding of the transitions leading to the formation of these phases is a challenging theoretical problem. A full understanding of these systems must necessarily involve some cooperative effects between molecules, and these may be quite dominant. Nevertheless a detailed understanding of the single molecule properties may yield considerable information about the orientational potential and the nature of the transitions. Provided that the molecule contains a sufficient fraction of protons, then incoherent neutron scattering experiments provide a very powerful means of achieving this. The proton has a very high and incoherent scattering cross section (*ca.* 80 b[¶] compared with a few barns for most other nuclei; e.g. *ca.* 5 b for C) so that, given enough protons, the incoherent scattering from these dominates the observed scattering and renders its interpretation relatively straightforward.

Another area in which such methods are very useful is in the study of intramolecular reorientations. In both cases there are two distinct experimental aspects: the inelastic spectrum gives information about the torsional or librational levels and the quasielastic spectrum about the stochastic jumping between different potential wells. The barrier heights between pocket states may be so weak compared with the thermal energy that the motion goes over to rotational diffusion with a more or less random distribution of orientation, but this is uncommon (Leadbetter & Lechner 1979; Hüller & Press 1978; Stiller 1978).

[‡] Present address: Chemistry Department, University of California, Berkeley, California 94720, U.S.A.
[¶] 1 barn (b) = 10^{-28} m^2.

At sufficiently low temperatures and for small enough moments of inertia, the rotational motions must be described in terms of quantum mechanical tunnelling states. In practice this tunnelling occurs only for H and D atoms so that only groups such as CH_4, NH_4^+ and $-CH_3$ are involved. The study of such tunnelling states is important for two reasons. First, they provide additional parameters for the detailed determination of the rotational potential, and secondly, they are necessary for an *explanation* of the reorientational processes compared with their mere description (Hüller & Press 1978, Clough & Heidemann 1979; Clough *et al.* 1978). Although these studies are not the subject of this paper, a brief discussion will be given because of their great importance to the understanding of rotational motions and because neutrons have recently come to play a major role in this work. The nature of the tunnelling states may be seen with reference to the schematic energy correlation diagram of figure 1. In the extreme of low orientational potential, the states are those for quantum mechanical free rotation while at the extreme of high potential they are librational (harmonic) oscillator states. The splitting of the librational states is the tunnel splitting and in many interesting cases it falls within the

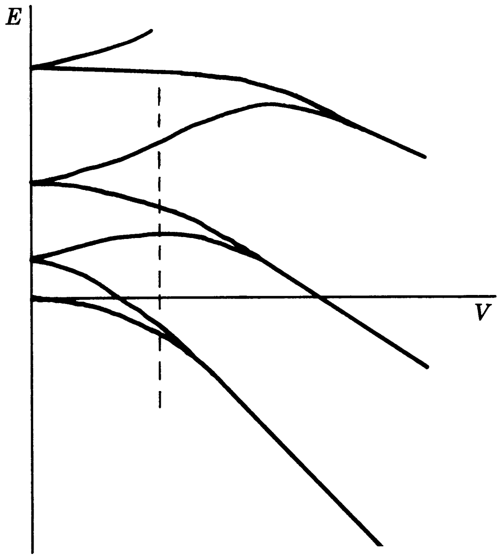

FIGURE 1. Energy level correlation diagram showing the relation between free rotation and vibrational levels for a system in an orientational potential of height V. The dashed line shows schematically a potential below which the tunnel splittings might be observable in a neutron experiment.

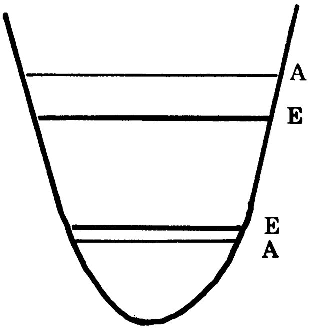

FIGURE 2. Energy diagram for threefold rotational system (e.g. $-CH_3$), showing the first two torsional levels with their tunnel splittings.

range accessible to neutron studies ($\Delta E \gtrsim 1$ µeV typically for $V \lesssim 400\ \text{cm}^{-1} \approx 50$ meV. The situation is shown in figure 2 for the $-CH_3$ case where the two lowest libration states are shown. Typical spectra for the ground state splitting as a function of T for this case are shown in figure 3 (after Batley *et al.* 1977), which shows how the tunnelling picture goes over at still relatively low temperature to one where a classical stochastic description of the reorientation is adequate.

A number of very elegant experiments have recently been performed on the study of the temperature and pressure dependence of tunnelling splittings and line widths for $-CH_3$ rotations, including measurements of the first excited torsional state (Clough & Heideman 1979; Clough *et al.* 1978, 1979) as well as a more complicated three-dimensionally rotating system (Prager *et al.* 1977; Press & Prager 1977; Prager & Alefeld 1976).

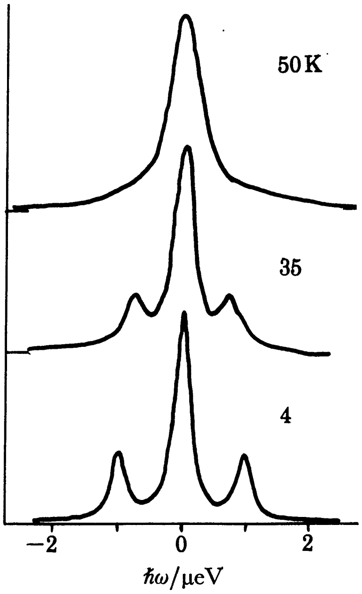

FIGURE 3. Typical neutron scattering tunnelling spectra (after Batley *et al.* 1977) for a $-CH_3$ group as a function of temperature, showing the change from tunnelling transitions at low T to classical quasielastic broadening at higher T.

2. INCOHERENT NEUTRON SCATTERING FROM MOLECULES UNDERGOING BOUND MOTIONS

A detailed review of this topic has recently been published by Leadbetter & Lechner (1979), so here it is necessary only to summarize a few important results.

First it is assumed that the molecules contain sufficient protons so that the total scattering from them is dominated by the incoherent cross section of the protons (except at Bragg reflections). The incoherent scattering law is then the time Fourier transform,

$$S_s(Q, \omega) = \tfrac{1}{2}\pi \int_{-\infty}^{\infty} \{\exp(-i\omega t)\}\, I_s(Q, t)\, dt,$$

of the intermediate scattering function

$$I_s(Q, t) = \exp\{i\boldsymbol{Q}\cdot\langle[\boldsymbol{r}(t) - \boldsymbol{r}_0(0)]\rangle\},$$

which may alternatively be written in terms of the conditional probability function $G_s(\boldsymbol{r}, \boldsymbol{r}_0, t)$ and the probability distribution $g(\boldsymbol{r}_0)$ of initial positions $\boldsymbol{r}_0$,

$$I_s(\boldsymbol{Q}, t) = \iint \exp \mathrm{i}\boldsymbol{Q}\cdot[\boldsymbol{r}-\boldsymbol{r}_0]\, G_s(\boldsymbol{r}, \boldsymbol{r}_0, t)\, g(\boldsymbol{r}_0)\, \mathrm{d}\boldsymbol{r}\, \mathrm{d}\boldsymbol{r}_0.$$

When the molecule contains dynamically non-equivalent protons, $S_s(\boldsymbol{Q}, \omega)$ must be averaged over them to give the scattering law for the molecule.

For bound motions such that the proton (molecule) is confined to a restricted volume of space, the long time limit of $G_s(\boldsymbol{r}, \boldsymbol{r}_0, t) = G_s(\boldsymbol{r}, \infty)$ may be separated out to give

$$I_s(\boldsymbol{Q}, t) = I_s(\boldsymbol{Q}, \infty) + I'_s(\boldsymbol{Q}, t),$$

and since $G_s(\boldsymbol{r}, \infty) = g(\boldsymbol{r}_0)$,

$$\begin{aligned} I_s(\boldsymbol{Q}, \infty) &= |\textstyle\int \{\exp(\mathrm{i}\boldsymbol{Q}\cdot\boldsymbol{r})\}\, G_s(\boldsymbol{r}, \infty)\, \mathrm{d}\boldsymbol{r}\,|^2 \\ &= |\langle \exp(\mathrm{i}\boldsymbol{Q}\cdot\boldsymbol{r}\rangle|^2 \\ &= A_0(\boldsymbol{Q}), \end{aligned} \tag{1}$$

and the scattering law becomes

$$S_s(\boldsymbol{Q}, \omega) = A_0(\boldsymbol{Q})\, \delta(\omega) + S'_s(\boldsymbol{Q}, \omega), \tag{2}$$

where $A_0(\boldsymbol{Q})$ is called the elastic incoherent structure factor (e.i.s.f.).

For a vibrational motion of frequency ω_0, (2) becomes

$$S_s(\boldsymbol{Q}, \omega) = \exp\langle(\boldsymbol{Q}\cdot\boldsymbol{u})^2\rangle\, \delta(\omega) + S_s^{\mathrm{inel}}(\boldsymbol{Q}, \omega), \tag{3}$$

where $A_0(\boldsymbol{Q})$ is now the well known Debye–Waller temperature factor and $S_s^{\mathrm{inel}}(\boldsymbol{Q}, \omega)$ comprises peaks at $\pm\hbar\omega_0$.

For bound stochastic motion, for example rotational motion about the centre of mass

$$S_s(\boldsymbol{Q}, \omega) = A_0(\boldsymbol{Q})\, \delta(\omega) + S_s^{\mathrm{qe}}(\boldsymbol{Q}, \omega), \tag{4}$$

where $A_0(\boldsymbol{Q})$ now depends on the geometrical nature of the rotations and examples are shown by the data in figures 6 and 7. $S_s^{\mathrm{qe}}(\boldsymbol{Q}, \omega)$ is a quasielastic scattering component that depends upon both the geometry and timescale of the rotations. Usually $I_s'^{\mathrm{R}}(\boldsymbol{Q}, t)$ will be of the general form

$$I_s'^{\mathrm{R}}(\boldsymbol{Q}, t) = \sum_{l=1} A(\boldsymbol{Q}) \exp(-t/\tau_l),$$

so that

$$S_s^{\mathrm{qe}}(\boldsymbol{Q}, \omega) = \sum_{l=1} A_l(\boldsymbol{Q})\, \mathscr{L}(1/\tau_l), \tag{5}$$

where

$$\mathscr{L}(1/\tau_l) = \pi^{-1}\, \tau_l^{-1}/(\tau_l^{-2}+\omega^2).$$

Here we shall be concerned mainly with such motions so that the observed scattering law will be of the form of (4) and (5). Typical examples are shown by the data of figures 4 and 5.

Detailed discussion of various examples may be found in Leadbetter & Lechner (1979) but we give here for illustration the results for three simple cases, because they are relevant to the case of *t*-butyl chloride (and the liquid crystals) discussed below.

Threefold jump reorientation

For a single crystal specimen,

$$\begin{aligned} S_s(\boldsymbol{Q}, \omega) = {} & [\tfrac{1}{3}+\tfrac{2}{9}(\cos \boldsymbol{Q}\cdot\boldsymbol{r}_{12}+\cos \boldsymbol{Q}\cdot\boldsymbol{r}_{23}+\cos \boldsymbol{Q}\cdot\boldsymbol{r}_{13})]\, \delta(\omega) + [\tfrac{2}{3}-\tfrac{2}{9}(\cos \boldsymbol{Q}\cdot\boldsymbol{r}_{12} \\ & +\cos \boldsymbol{Q}\cdot\boldsymbol{r}_{23}+\cos \boldsymbol{Q}\cdot\boldsymbol{r}_{13})]\, \mathscr{L}(\tfrac{2}{3}\tau), \end{aligned} \tag{6}$$

where τ is the residence time (τ^{-1} the jump probability) and 1, 2 and 3 label the sites. For a powder this becomes (for equidistant sites)

$$S_s(Q,\omega) = [\tfrac{1}{3}+\tfrac{2}{3}j_0(Qa\surd 3)]\,\delta(\omega)+(\tfrac{2}{3}-\tfrac{2}{3}j_0(Qa\surd 3)]\,\mathscr{L}(\tfrac{2}{3}\tau), \tag{7}$$

where a is the radius of the circle on which the sites are located and $j_0(x)$ is the zero order spherical Bessel function ($j_0(x) = x^{-1}\sin x$). Most quasielastic studies of molecular reorientations so far have been made on powder samples, but notable exceptions are studies on orientated liquid crystal samples described briefly below.

Rotation on a circle

The above result (equation (7)) has been extended to the general case of m equidistant sites on a circle of radius a (Barnes 1973) for a powder sample, when

$$S_s(Q,\omega) = A_0(Q)\,\delta(\omega)+\sum_{l=1}^{l=m} A_l(Q)\,\mathscr{L}(\tau_l^{-1}), \tag{8}$$

where
$$A_l(Q) = m^{-1}\sum_{j=1}^{m} j_0\{2Qa\sin(\pi j/m)\}\cos(2\pi lj/m) \tag{9}$$

and
$$\tau_l = \tfrac{1}{2}\tau/\{\sin^2(\pi l/m)\}. \tag{10}$$

For $m\rightarrow\infty$, these results are equivalent to continuous rotational diffusion on the circle with $D_r = \tau_1^{-1}$ (Dianoux *et al.* 1975).

Rotational diffusion on a sphere of radius a

$$S_s(Q,\omega) = j_0^2(Qa)\,\delta(\omega)+\sum_{l=1}^{\infty}(2l+1)\,j_l^2(Qa)\,[l(l+1)\,D_r]. \tag{11}$$

D_r is the rotational diffusion constant and j_0 a spherical Bessel function.

Translational diffusion

When continuous centre-of-mass diffusion occurs the scattering law becomes a Lorentzian of argument $D_t Q^2$ where D_t is the translational diffusion coefficient. Because low Q data probe the large distance components of motion ($A_0(Q)\rightarrow 1$ as $Q\rightarrow 0$), then measurements at low enough Q enable D_t to be determined even if the molecule is also rotating. The separation of the rotational motion from translation at high Q depends on the relative magnitudes of $D_t Q^2$ and τ_l^{-1}: the effect of translational motion being to broaden, by folding with $\mathscr{L}(D_t Q^2)$, the scattering laws discussed above. Examples of cases where such separation is possible will be discussed below for liquid crystals.

3. TERTIARY BUTYL CHLORIDE, $(CH_3)_3CCl$

3.1. *Introduction*

This is an excellent example for illustrating the use of high resolution incoherent neutron quasielastic scattering (i.n.q.e.s.) techniques because, despite a great amount of work, particularly with other techniques, the nature of the molecular disorder in the three solid phases is still not clearly established. The phase behaviour is as follows:

$$\text{crystal III} \xrightleftharpoons{183\ \text{K}} \text{crystal II (tetragonal)} \xrightleftharpoons{219\ \text{K}} \text{crystal I (cubic)} \xrightleftharpoons{247\ \text{K}} \text{liquid.}$$

Crystal III is an ordered phase whose detailed structure has not yet been published. Crystal II is tetragonal (Rudman & Post 1968), and crystal structure determination suggested a head-to-tail packing of molecules having collinear C–Cl and random orientation of methyl groups about this axis. Crystal I is f.c.c. with the molecules having non-random but undetermined orientations (Schwartz *et al.* 1951). These structural results are in accord with dielectric (Kushner *et al.* 1950) and n.q.r. (O'Reilly *et al.* 1973) measurements which indicate tumbling of the C–Cl axis in I but not in II and with calculations and for i.r. absorption data of Lassier & Brot (1968) suggesting favoured sites in I comprising a manifold of cubic symmetry. Some recent relatively low resolution i.n.q.e.s. results (Goyal *et al.* 1974) on phase II were interpreted as most consistent with threefold reorientations about the dipole axis, whereas later measurements (Larsson *et al.* 1978; Mansson & Larsson 1977) were interpreted as showing rotation about all axes in II as well as I, although that about the dipole axis was some 9 times faster than in the other directions, all molecular rotation being frozen in III. This result for II disagrees with deductions from other experiments (above).

A very detailed nuclear magnetic resonance study was carried out by O'Reilly *et al.* (1973) in which it was concluded, on the basis of spin lattice relaxation (T_1 and $T_{1\rho}$) measurements, that in solid III the rates of methyl reorientations about their symmetry axes obey an Arrhenius law: $\tau = \tau_0 \exp(E_a/kT)$ with $E_a = 15.2$ kJ mol^{-1} and $\tau_0 = 7.3 \times 10^{-15}$ s. Another motion on a time scale of 10^{-7} to 10^{-8} s, in crystal II and III, was identified as a reorientation of the whole molecule about the C–Cl axis. These conclusions are inconsistent with the results of detailed i.n.q.e.s. and neutron inelastic (i.n.i.s.) scattering experiments on the closely related compound, *t*-butyl cyanide (Frost 1979; Frost *et al.* 1980). For this substance the molecules reorientate about the dipolar axis even in the lowest temperature phase with $\tau \approx 10^{-10}$ s, and as the temperature increases this process rapidly becomes much faster than the methyl reorientation which, from the methyl torsion frequencies and direct i.n.q.e.s. observations, can be characterized by an Arrhenius law ($E_a = 16.3$ kJ mol^{-1}, $\tau_0 = 0.20 \times 10^{-12}$ s). As both compounds have similar methyl torsional frequencies (Durig *et al.* 1969; Ratcliffe & Waddington 1976) the methyl reorientation correlation times should be similar and hence much longer than those deduced from the n.m.r. experiments, which also give an unphysically high value for τ_0.

We have therefore made new measurements at 165, 202 and 236 K, i.e. one measurement in each solid phase, using the time-of-flight multi-chopper spectrometer (IN5) at the Institut Laue–Langevin, Grenoble. The sample was contained in a stainless steel can and had a thickness of *ca.* 0.3 mm. The incident wavelength of 7.8 Å† gave the experiment an elastic momentum transfer range of 0.35 to 1.47 Å^{-1} and an elastic energy resolution (f.w.h.m.) of *ca.* 31 μeV. The spectra obtained were transformed by using well known procedures to the scattering law $S_s(Q, \omega)$. The results for crystal III showed no quasielastic broadening indicating that any random molecular motions (intramolecular or intermolecular reorientations) are slower than 3×10^{-10} s. The results for crystals II and I are shown respectively in figures 4 and 5 at three different Q values and the experimental e.i.s.f. data are plotted in figures 6 and 7. These were obtained by using a least squares computer fit and equations of the form of (4) and (5). The determination of reliable e.i.s.f. values from IN5 is facilitated because of the triangular shape of the resolution function.

† 1 Å = 10^{-10} m = 10^{-1} nm.

3.2. *Crystal II*

The spectra for II clearly show an elastic peak superimposed on a broadened component with a full width at half maximum of 360 μeV (implying a correlation time of *ca.* 4×10^{-12} s). The slower motion observed by the n.m.r. experiment in this phase (and attributed to uniaxial molecular reorientation) is far too slow to give any detectable broadening, as is translational diffusion. Because of instrumental difficulties in measuring $T_{1\rho}$, O'Reilly *et al.* (1973) could not determine correlation times for the faster motion in this phase, but from their data in solid I and III this time must lie between *ca.* 10^{-10} and *ca.* 6×10^{-12} s. It seems certain therefore that the n.m.r. and i.n.q.e.s. experiments relate to the same fast motion but the experimental e.i.s.f. shows that this motion is definitely *not* ~~a~~ reorientation of the methyl groups as suggested by O'Reilly *et al.* Instead it is much more closely related to rotational diffusion of the whole

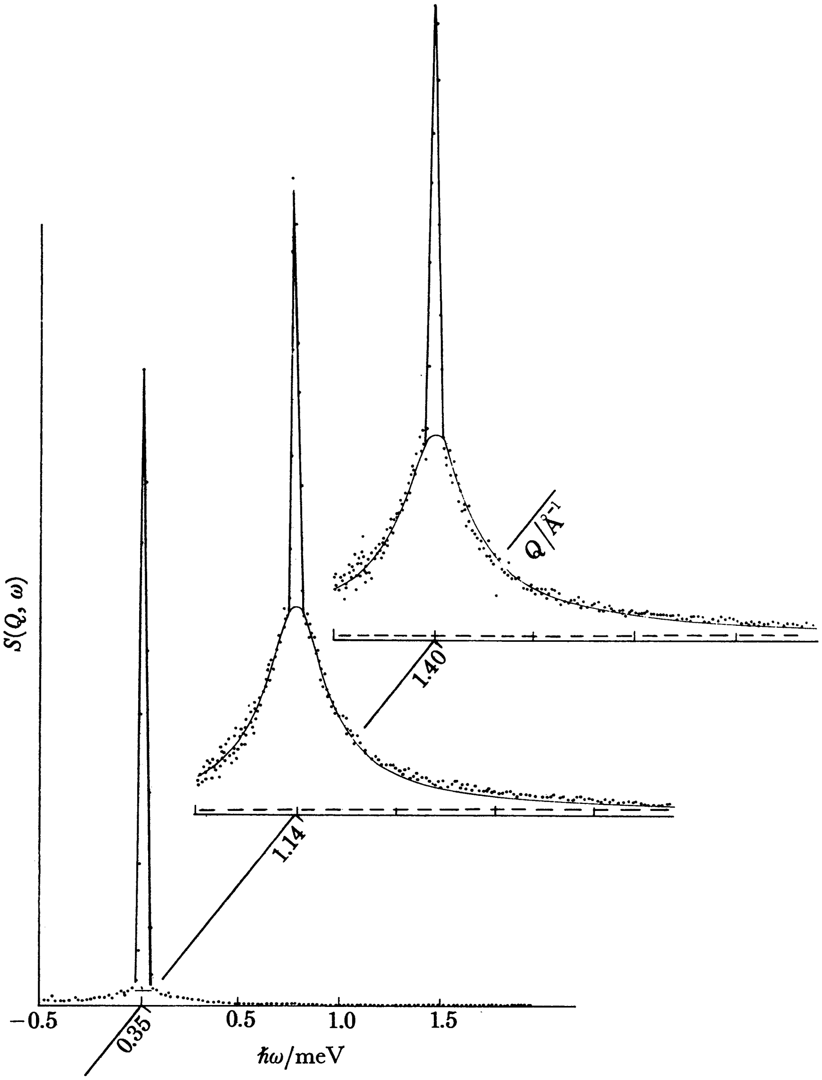

FIGURE 4. Typical neutron spectra for the crystal II phase of *t*-butyl chloride at 202 K. The full line represents a fit to the data of the uniaxial rotation model (equation (8); $m \gtrsim 6$), but with the coefficient of the elastic peak a fittable parameter. This gives the e.i.s.f. of figure 6. The dashed line shows the inelastic background.

molecule about the C–Cl axis. The e.i.s.f. for the model of simple uniaxial rotational diffusion ($m \gtrsim 6$ (equation (8)), with the use of known molecular geometry) is shown in figure 6.

The experimental e.i.s.f. is in fact lower than that for uniaxial rotational diffusion, even when multiple scattering is taken into account (figure 6) which was done with the use of a Monte Carlo method (Johnson 1974). This shows that the motion must be even less restricted than just random rotation about the C–Cl axis. Reorientations of the methyl groups might cause this but in fact they are too slow to make a significant contribution to the quasielastic broadening and hence to have been seen in the present experiments (see below). Therefore there must be motions of the molecule about its other axes, although these must be much more localized than overall rotation. Another possibility is that as a molecule lacks the room to rotate freely about any axis, and the molecular and (average) site symmetries are different (Lassier & Brot 1968), then such a reorientation may be accompanied by a lateral

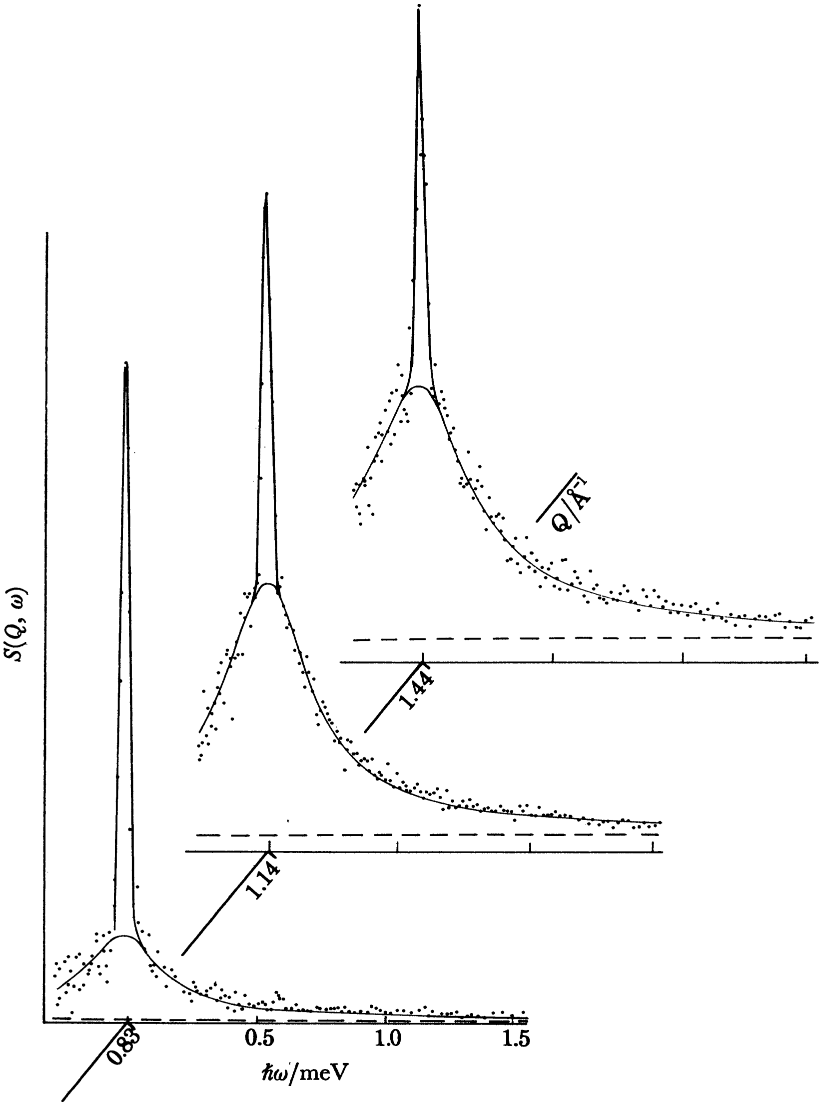

FIGURE 5. Typical neutron spectra for the crystal I phase of *t*-butyl chloride at 236 K. The full line shows the fit to the data of the model for random rotational diffusion on a sphere (equation (11)).

relaxation of the neighbouring molecules. The e.i.s.f. may be fitted by a variety of similar models for the limited Q range of these experiments and it is not possible to distinguish between them without additional evidence. Two examples are shown in figure 4: (i) a small step uniaxial diffusion (equation (8) with $m \gtrsim 6$) plus a random lateral displacement of the protons with $\langle x^2\rangle^{\frac{1}{2}} \approx 0.7$ Å; (ii) threefold uniaxial rotation plus random fluctuations of the dipolar axis (Volino *et al.* 1976) with $\langle \cos\theta\rangle = 0.75(\bar{\theta} \approx 40°)$. Furthermore, the width of the quasi-elastic spectrum increases with Q, showing the presence of at least two Q-dependent components.

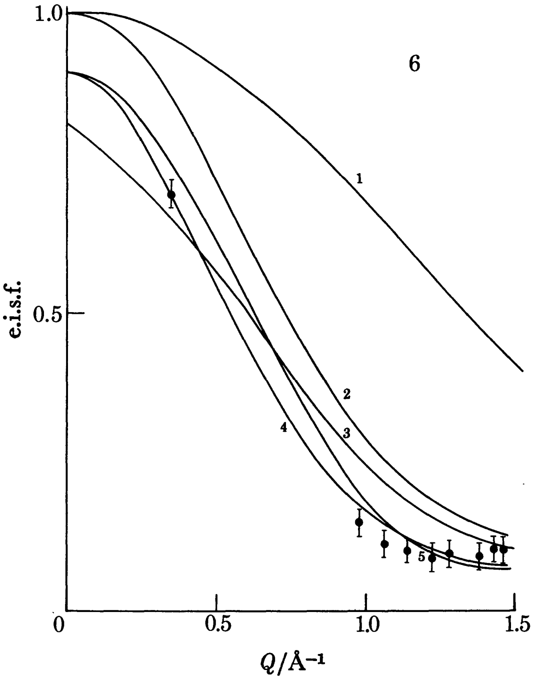

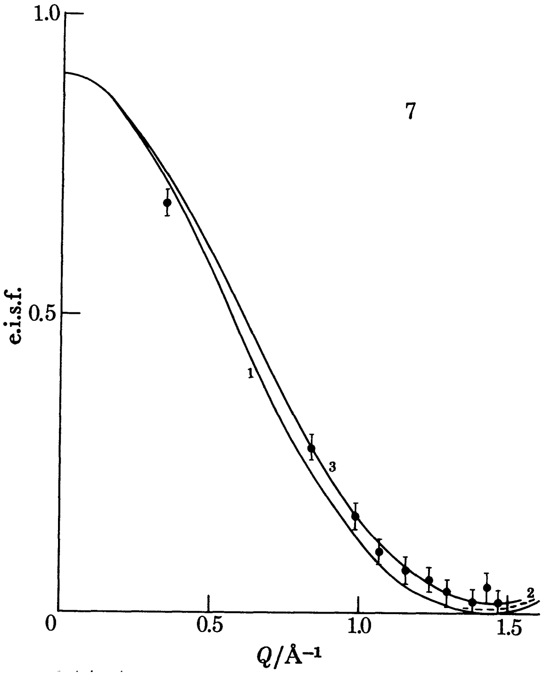

FIGURE 6. The elastic incoherent structure factor (e.i.s.f.) for *t*-butyl chloride at 202 K. The points are experimental values. The lines are the e.i.s.f. expected from the following models: (1) threefold jump reorientation of the methyl groups; (2) uniaxial rotational diffusion about the C–Cl axis; (3) as (2), but with the ***maximum possible*** correction for multiple scattering; (4) threefold jump reorientation about the C–Cl axis plus *ca.* 40° fluctuations of the long axis orientation and including the best estimate of multiple scattering effects; (5) uniaxial rotational diffusion plus a random lateral displacement of the molecule with $\langle x^2\rangle^{\frac{1}{2}} \approx 0.7$ Å and including multiple scattering effects.

FIGURE 7. The elastic incoherent structure factor (e.i.s.f.) for the crystal I phase of *t*-butyl chloride at 236 K. ●, Experimental. The lines are calculated for the following models, including the effects of multiple scattering: (1) random rotational diffusion; (2) reorientations of C–Cl to point to all eight corners of a cube plus rotation around the C–Cl axis; (3) reorientations of C–Cl to point to the four corners of a tetrahedron plus rotation around the C–Cl axis (see text).

This can be fitted by a small step rotational motion as shown in figure 4, which would then imply that the additional displacements are on a similar time scale, or alternatively by a threefold rotation (perhaps in a softened potential; Dianoux & Volino 1977) together with the additional motion on a slightly different time scale. In either case, the data are consistent with uniaxial reorientation with a correlation time of about 4×10^{-12} s, and an additional motion is revealed which is either associated with a cooperative relaxation involving steric effects and changes of local symmetry, or overdamped fluctuations of the C–Cl axis which presage the molecular tumbling observed in the high temperature crystal I. We believe the latter to be the dominant motion because it is more consistent with the X-ray structural results and the small change of dielectric constant at the III–II transition.

The interpretation of the n.m.r. results must therefore be changed (and there seems to be no difficulty about this) so that the faster motion is the uniaxial whole-molecular rotation discussed above, while the slower motion must be the methyl reorientation. In this case the n.m.r. experiments suggest for the methyl reorientation $\tau/\mathrm{s} = (7 \pm 5) \times 10^{-12} \exp{(11.7 \pm 0.9)}\ \mathrm{kJ\ mol^{-1}}/RT$. From methyl torsion frequencies, Ratcliffe & Waddington (1976) estimate a barrier height $V = 18.5\ \mathrm{kJ\ mol^{-1}}$; evaluating an average activation energy for reorientation gives $E \gtrsim 17\ \mathrm{kJ\ mol^{-1}}$. Such discrepancies are, however, not uncommon and probably imply that the assumed potential is inadequate. The pre-exponential factor, on the other hand, is now reasonable, being of the order of the thermal free rotator correlation time (Brot 1969). Furthermore, an Arrhenius behaviour is expected for the methyl reorientation, with not much change through the transitions, because the barrier to reorientation is largely internal and therefore not strongly temperature dependent. This is certainly not true for motion about the C–Cl axis since, as we have demonstrated for pivalonitrile (Frost *et al.* 1980), and as the n.q.r. data of O'Reilly *et al.* (1973) suggest; the barrier hindering this motion is changing rapidly near the transitions. Consequently the activation energy and pre-exponential factor given by O'Reilly *et al.* for this motion (but assigned to methyl reorientation) are not very meaningful.

3.3. *Crystal I*

For crystal I the e.i.s.f. data (figure 7) are in reasonable agreement with the unequivocal quadrupole resonance, microwave absorption (see below) and p.m.r. linewidth results that the molecules are tumbling with at least cubic symmetry. Both the e.i.s.f. and $S_s(Q, \omega)$ itself are fitted quite well by the simple model for rotational diffusion (equation (11)) with a best fit value for D_r^{-1} at 236 K of 8×10^{-12} s. The dielectric relaxation measurements give a value for the first spherical harmonic correlation time $\tau_1 = 5.4 \times 10^{-12}$ s (Brot & Lassier-Govers 1976) which may be compared with $(2D_r)^{-1} = 4 \times 10^{-12}$ s and the n.m.r. spin lattice relaxation measurements give the second spherical harmonic correlation time $\tau_2 = 3 \times 10^{-12}$ s which should be compared with $(6D_r)^{-1} = 1.3 \times 10^{-12}$ s. The agreement is fair, but together with analysis of dielectric (Lassier & Brot 1968) and X-ray data suggests that the tumbling is not entirely free but that weak minima occur in the orientational potential. Such a localization should give rise to a higher e.i.s.f., and indeed the experimental points are higher than expected for rotational diffusion: the difference is small but significant. The most likely orientations are those in which the site symmetry and the molecular symmetry have common elements, and Lassier & Brot have discussed the energies of the various possible orientations and the barriers between them.

The restricted range of Q and the single temperature for the present experiments does not permit a full analysis of the reorientations, but do enable us to identify the fastest motions. Thus the n.q.r. data, unit cell symmetry (f.c.c.) and entropy changes imply that on the time scale of the n.q.r. experiment (10^{-7} s), the C–Cl axis can point to at least the eight corners of the cubic cell (the molecular C_3 axis then coinciding with the crystal C_3 axis). The e.i.s.f. for this manifold is shown in figure 7 and is almost identical (for $Q \gtrsim 1.5$ Å^{-1}) to that for random orientation, showing that the motion on the neutron time scale is more restricted than this. Since the rapid reorientation of the molecule about its C_3 axis must certainly occur in I as well as in II, perhaps the most likely additional rapid reorientation is rotation of the pseudo-tetrahedron about the C_3 axes of the methyl groups. The e.i.s.f. for this total motion, which moves the C–Cl axis among the four corners of the pseudo-tetrahedron, is in perfect agreement with the data when corrected for multiple scattering. This implies that the C_4 rotations of the pseudo-tetrahedron (and any other motions) are slower than *ca.* 10^{-10} s. The data cannot distinguish whether the rotation about the C–Cl axis in I is threefold or by small steps, but it may be concluded that this motion is not more than about three times faster than the reorientation of the C–Cl axis among its four orientations, and the reorientation frequencies are in the range $1–5 \times 10^{11}$ rad s^{-1}.

3.4. *Conclusion*

The ability of i.n.q.e.s. to probe spacial as well as temporal aspects of the molecular motions has permitted unequivocal identification to be made of the basic type of reorientational motions taking place in the two disordered crystal phases of *t*-butyl chloride and determination of their correlation times. Differences from a previous neutron scattering study may be attributed to the better resolution of the present experiments. The results show clearly that whole molecule reorientation is more rapid than that of C_3 methyl group reorientation, in agreement with deductions from torsional frequencies, and show further that the two types of motion in II and I were wrongly identified in n.m.r. experiments.

4. Liquid crystals

4.1. *Introduction*

Thermotropic liquid crystals are intermediate phases that are often found between the normal solid and liquid phases of pure compounds. (A second type, lyotropics, are formed by surfactant molecules in concentrated solution, but these are not discussed here.) Liquid crystals are invariably made up of elongated, lath-like molecules, and as the temperature of a sample is increased the ordered solid phase changes to one or more different mesophases before the isotropic liquid is reached. Such behaviour is found in many organic compounds (see, for example, Gray 1979). A typical example, known as IBPBAC, has been chosen to illustrate how quasielastic neutron scattering has been used to study the mesophases. The molecular structure, chemical name and transition temperatures of IBPBAC are given below.

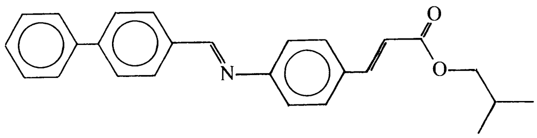

isobutyl 4-(4′-phenylbenzylidineamino)-cinnamate

$$\text{crystal} \underset{\text{supercools}}{\overset{86\ ^{\circ}\mathrm{C}}{\rightleftharpoons}} \text{smectic E} \overset{114\ ^{\circ}\mathrm{C}}{\rightleftharpoons} \text{smectic B} \overset{162\ ^{\circ}\mathrm{C}}{\rightleftharpoons} \text{smectic A} \overset{206\ ^{\circ}\mathrm{C}}{\rightleftharpoons} \text{nematic} \overset{214\ ^{\circ}\mathrm{C}}{\rightleftharpoons} \text{isotropic liquid}$$

Figure 8 shows schematically that the nematic phase has only orientational order of the long molecular axes, but the smectic phases are characterized by a layer structure. The different smectic phases are distinguished by the degree of orientational ordering about the long axes, the interlayer correlation and in some cases (but not IBPBAC) a tilt of the molecules with respect to the layers. X-ray diffraction experiments (see, for example, Doucet (1979) and Leadbetter *et al.* (1979*a*)) have shown that the packing is liquid-like in S_A layers, hexagonal on average in S_B layers and there is a herringbone packing of the lath-like molecules in the S_E layers. The director, $\boldsymbol{n}$, is defined as the mean direction of the long axes in a liquid crystal. Monodomain samples may be prepared by carefully melting a single crystal or by cooling a magnetically aligned nematic phase.

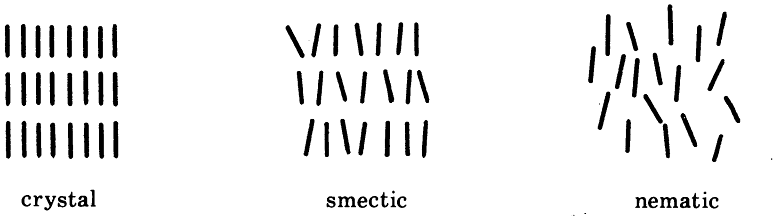

Figure 8. Schematic view of the long molecular axis in the liquid crystalline phases of IBPBAC.

4.2. *Principle of the measurements*

The techniques used to study *t*-butyl chloride have also been used to elucidate the dynamics of several liquid crystal phases (Leadbetter *et al.* 1979*b*; Leadbetter & Richardson 1978, 1979). Incoherent quasielastic neutron scattering measurements have been used to observe and quantify the slow diffusive molecular motions of IBPBAC in its liquid crystalline phases, with the aim of achieving a better understanding of molecular interactions in these phases. A version of IBPBAC with deuterated isobutyl groups was used so that the results would be dominated by incoherent scattering from protons on the relatively rigid core of the molecule.

Great advantage can be taken from the fact that measurements can be done on aligned samples with $\boldsymbol{Q}$ parallel or perpendicular to $\boldsymbol{n}$. For example, if the molecules are undergoing uniaxial rotational diffusion the scattering law is given by the formula

$$S(\boldsymbol{Q},\omega) = J_0^2(Qa\sin\theta)\,\delta(\omega) + \pi^{-1}\sum_{l=1}^{\infty} J_l^2(Qa\sin\theta)\,\frac{l^2D_r}{(l^2D_r^2)^2+\omega^2},$$

where J_l is the lth cylindrical Bessel function, a is the radius of gyration of a proton, θ is the angle between $\boldsymbol{Q}$ and $\boldsymbol{n}$, and D_r is the rotational diffusion constant.

Two extremes for the e.i.s.f. would be observable in an aligned sample:

$$\text{for}\quad \boldsymbol{Q}\perp\boldsymbol{n},\ \text{e.i.s.f.}_{\perp} = J_0^2(Qa);$$

$$\text{for}\quad \boldsymbol{Q}\parallel\boldsymbol{n},\ \text{e.i.s.f.}_{\parallel} = 1.$$

If the uniaxial rotational diffusion is restricted by some preferred orientations of the molecules, then the e.i.s.f.$_{\perp}$ will be higher than that given above (for $Qa < 3$).

The presence of an additional motion on the same timescale with an appreciable amplitude perpendicular to $\boldsymbol{n}$, such as directional fluctuations of the long molecular axes, will tend to decrease the e.i.s.f.$_{\perp}$. Any diffusive motion parallel to $\boldsymbol{n}$ will result in the e.i.s.f.$_{\parallel}$ being reduced from unity. For instance, if the molecules undergo a random displacement parallel to $\boldsymbol{n}$ with a Gaussian 'infinite time' distribution about their mean positions, the e.i.s.f.$_{\parallel}$ would be given by the formula

$$\text{e.i.s.f.}_{\parallel} = \exp\left(-Q^2\langle Z^2\rangle\right), \tag{12}$$

where $\langle Z^2\rangle^{\frac{1}{2}}$ is the r.m.s. amplitude of the displacement. These different motions can be distinguished by measurements on aligned liquid crystalline samples.

The above equations illustrate the general principle that for any localized motion, the scattering becomes entirely elastic as Q tends to zero:

$$S(\boldsymbol{Q}, \omega) = \delta(\omega);$$

$$Q \rightarrow 0.$$

At sufficiently low Q, only translational diffusion will broaden the profile of the scattered neutrons. However, at low Q, the broadening from translational diffusion is very small and so very high resolution is necessary to observe it. There are therefore two types of experiment that have been done on liquid crystals:

(i) very high resolution measurements over a narrow energy transfer range at low Q, to give information about translational diffusion;

(ii) high resolution measurements over a wider energy transfer and Q range, to give information on the localized motions, such as rotation.

4.3. *Translational diffusion*

The IN10 high-resolution backscattering spectrometer at I.L.L., Grenoble, achieves a resolution of 1 μeV and covers an energy range of $|\hbar\omega| < 15$ μeV. In principle, translational diffusion constants parallel and perpendicular to $\boldsymbol{n}(D_{\parallel}, D_{\perp})$ can be obtained by measuring the Lorentzian broadening of the incident monoenergetic beam at $Q \ll 2\pi/d$ where d is the appropriate molecular dimension (cf. §2).

Figure 9 shows the diffusion constants of an aligned sample of IBPBAC in its liquid crystalline phases. Measurements were made at $0.14\ \text{Å}^{-1} < Q < 0.31\ \text{Å}$ and so the condition that $Q \ll 2\pi/d$ was well satisfied for $\boldsymbol{Q} \perp \boldsymbol{n}$ (where $d \approx 5$ Å, the molecular diameter) but not for $\boldsymbol{Q} \parallel \boldsymbol{n}$ (where $d \approx 27$ Å, the molecular length). The observed values of $D_{\parallel}$ in the S_A phase are therefore expected to be overestimates since the molecule is only followed for a distance that is comparable to its length. However, a detailed analysis (Richardson *et al.* 1980) has shown that the layers in the S_A only offer a weak barrier to diffusion and so the measured values of $D_{\parallel}$ are within 40 % of the correct values. The discontinuous jump in $D_{\parallel}$ at the smectic A to nematic transition reflects the disappearance of this barrier. In the smectic B phase the broadening was hardly observable with the available resolution and so the diffusion constants are best regarded as upper limits.

4.4. *Localized molecular motions*

The IN5 multichopper spectrometer (resolution typically 20 μeV) has been used to observe the quasielastic scattering from localized diffusive molecular motions, which, in liquid crystals, are more rapid than translational diffusion. Measurements have been made on IBPBAC in all three of its smectic phases and converted into experimental e.i.s.f. values. In the S_E and S_B phases the translational diffusion is too slow to broaden the instrumental resolution, but in the S_A both the elastic and quasielastic components were broadened by an amount ΔE ($\Delta E = 2\hbar D_\text{t} Q^2$) predicted by the translational diffusion constant measured on IN10. Figure 10 shows typical quasielastic scattering spectra from IBPBAC at 150 °C in the S_B phase. Surprisingly, there is more quasielastic scattering for $\boldsymbol{Q} \parallel \boldsymbol{n}$ than for $\boldsymbol{Q} \perp \boldsymbol{n}$, and the low e.i.f.s.$_{\parallel}$ (figure 11) indicates that there is a localized motion (on a timescale faster than 10^{-10} s) parallel to $\boldsymbol{n}$ (i.e. perpendicular to the smectic layers). The amplitude of the motion can be found by fitting the e.i.f.s.$_{\parallel}$ predicted by (12) to the observed e.i.s.f.$_{\parallel}$. The same motion has been found to increase smoothly from 1 Å at 100 °C in the S_E phase to 1.8 Å at 150 °C in the S_B, before dropping slightly to 1.3 Å in the S_A. The e.i.s.f.$_\perp$ in the S_B lies between that expected for uniaxial rotational diffusion and jump reorientation by π and so the molecules must undergo some form of reorientation between six (or more) sites (with $\tau \approx 3 \times 10^{-11}$ s), but with some sites preferred over others. In the S_E phase the e.i.s.f.$_\perp$ was found to be higher than that expected for reorientation by π and so the molecules can only be undergoing some overdamped libration about their long axes with an amplitude of *ca.* 40°. In the S_A phase, the e.i.s.f.$_\perp$ is low enough to be in good agreement with that for uniaxial rotational diffusion about the long molecular axes plus small-amplitude directional fluctuations of these axes. The width of the quasielastic part of the scattering implies a rotational diffusion constant, D_r of 4.7×10^{10} rad^2 s^{-1}.

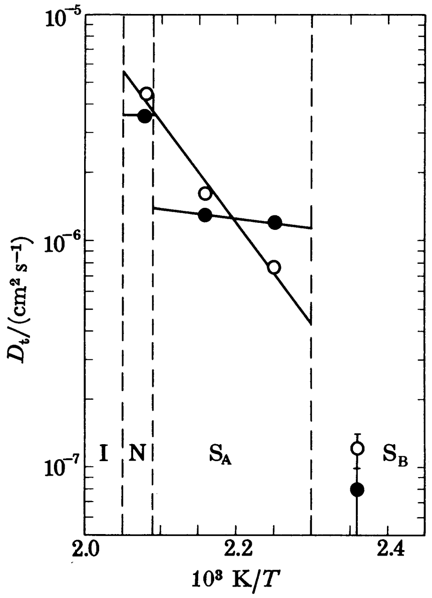

FIGURE 9. The translational diffusion constants of IBPBAC as measured by neutron scattering (●, $D_\parallel$; ○, $D_\perp$) as a function of inverse temperature. The lines serve to emphasize the discontinuity in $D_\parallel$ at the smectic A–nematic transition.

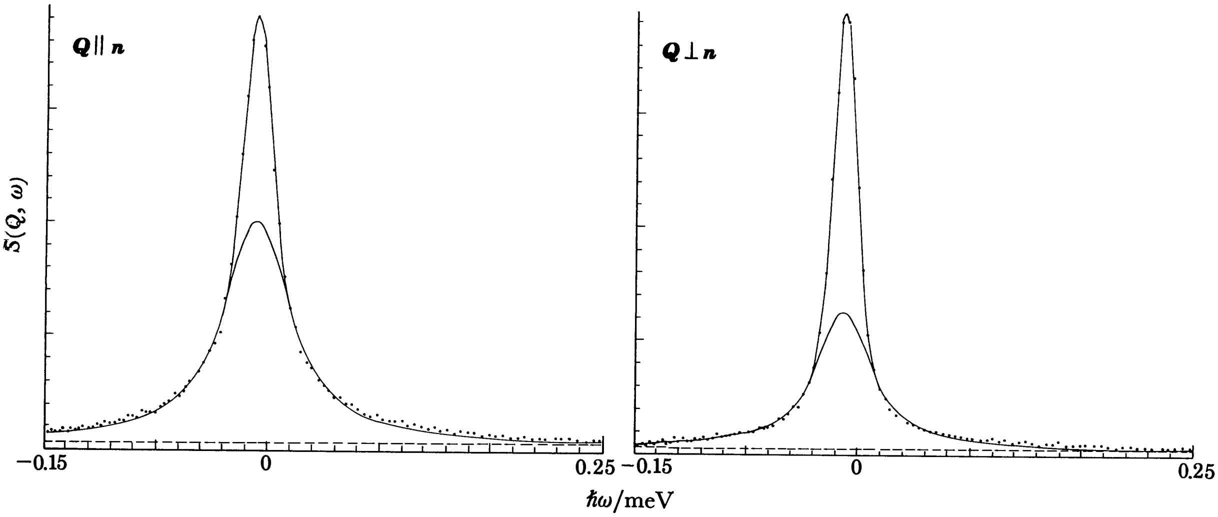

FIGURE 10. Quasielastic scattering from IBPBAC at 150 °C in the smectic B phase at $Q = 0.83$ Å^{-1} for $\boldsymbol{Q} \perp \boldsymbol{n}$ and $\boldsymbol{Q} \parallel \boldsymbol{n}$.

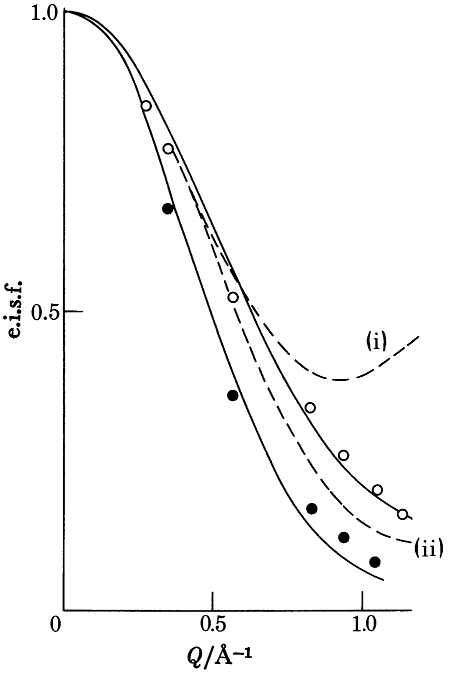

Figure 11. Elastic incoherent structure factors for IPBBAC. The experimental values for the smectic B phase at 150 °C are shown as points (●, $\boldsymbol{Q} \parallel \boldsymbol{n}$; ○, $\boldsymbol{Q} \perp \boldsymbol{n}$). The dashed lines are the e.i.s.fs expected for $\boldsymbol{Q} \perp \boldsymbol{n}$ if the molecules undergo (i) rotational diffusion or (ii) jump reorientation by π about their long axes. The solid lines are the result of fitting a model of restricted rotation plus a localized motion perpendicular to the layers in an imperfectly aligned sample to all the experimental data points.

4.5. *Summary*

These results from IBPBAC show how the dynamic rotational disorder about the long molecular axes changes along the S_E, S_B, S_A progression. Similar results from other substances have also extended this progression to the nematic phase. However, an important characteristic of all these phases appears to be that the molecules have the freedom to shuffle 1–2 Å parallel to their long axes (with $\tau < 10^{-10}$ s), and so any description of these phases entirely in terms of rotational disorder must be inadequate. The ability of molecules to move parallel to their long axes provides a mechanism by which some phase transitions take place (Leadbetter *et al.* 1979*c*). Certain liquid crystals have been found that undergo a smectic B to smectic H transition, not by a cooperative tilt of the molecules with respect to the layers but by a shift (at constant orientation) of 3–4 Å parallel to neighbouring molecules.

References (Frost *et al.*)

Barnes, J. D. 1973 *J. chem. Phys.* **58**, 5193–5201.
Batley, M., Thomas, R. K., Heidemann, A., Overs, A. H. & White, J. W. 1977 *Molec. Phys.* **6**, 1771–1778.
Brot, C. 1969 *Chem. Phys. Lett.* **3**, 319–322.
Brot, C. & Lassier-Govers, B. 1976 *Ber. BunsenGes. phys. Chem.* **80**, 31–41.
Clough, S. & Heidemann, A. 1979 *J. Phys.* C **12**, 761–770.
Clough, S., Alefeld, B. & Suck, J. B. 1978 *Phys. Rev. Lett.* **41**, 124–128.
Clough, S., Heidemann, A. & Kraxenberger, H. 1979 *Phys. Rev. Lett.* **42**, 1298–1301.
Dianoux, A. J. & Volino, F. 1977 *Molec. Phys.* **34**, 1263–1277.
Dianoux, A. J., Volino, F. & Hervet, H. 1975 *Molec. Phys.* **30**, 1181–1194.
Doucet, J. 1979 In *The molecular physics of liquid crystals* (ed. G. R. Luckhurst & G. W. Gray), pp. 317–341. London: Academic Press.

Durig, J. R., Craven, S. M. & Bragin, J. 1969 *J. chem. Phys.* **51**, 5663–5673.
Frost, J. C. 1979 Ph.D. thesis, University of Exeter.
Frost, J. C., Leadbetter, A. J. & Richardson, R. M. 1980 *Faraday Discuss. chem. Soc.* **69**. (In the press.)
Goyal, P. S., Nawrocik, N., Urban, S., Domoslawski, J. & Natkaniec, I. 1974 *Acta phys. pol.* A **46**, 399–406.
Gray, G. W. 1979 In *The molecular physics of liquid crystals* (ed. G. R. Luckhurst & G. W. Gray), pp. 1–29. London: Academic Press.
Hüller, A. & Press, W. 1978 In *Neutron inelastic scattering*, vol. 1, pp. 231–253. Vienna: I.A.E.A.
Johnson, M. W. 1974 *A.E.R.E. Rep.* no. 7682.
Kushner, L. M., Crowe, R. W. & Smyth, C. P. 1950 *J. Am. chem. Soc.* **72**, 1091–1098.
Larsson, K. E., Mansson, T. & Olsson, L. G. 1978 In *Neutron inelastic scattering*, Vol. 2, pp. 435–469. Vienna: I.A.E.A.
Lassier, B. & Brot, C. 1968 *J. Chim. phys.* **65**, 1723–1732.
Leadbetter, A. J. & Lechner, R. E. 1979 In *The plastic crystalline state* (ed. J. N. Sherwood), pp. 285–320. London: John Wiley.
Leadbetter, A. J. & Richardson, R. M. 1978 *Molec. Phys.* **35**, 1191–1200.
Leadbetter, A. J. & Richardson, R. M. 1979 In *The molecular physics of liquid crystals* (ed. G. R. Luckhurst & G. W. Gray), pp. 451–483. London: Academic Press.
Leadbetter, A. J., Frost, J. C., Gaughan, J. P. & Mazid, M. A. 1979*a* *J. Phys., Paris* **40**, 185–192.
Leadbetter, A. J., Frost, J. C. & Richardson, R. M. 1979*b* *J. Phys., Paris* **40**, C3–125.
Leadbetter, A. J., Kelly, B. A., Mazid, M. A., Goodby, J. W. & Gray, G. W. 1979*c* *Phys. Rev. Lett.* **43**, 630–633.
Mansson, T. & Larsson, K. E. 1977 *J. chem. Phys.* **67**, 4996–5005.
O'Reilly, D. E., Peterson, E. M., Scheie, C. E. & Seyfarth, E. 1973 *J. chem. Phys.* **59**, 3576–3584.
Prager, M. & Alefeld, B. 1976 *J. chem. Phys.* **65**, 4927–4928.
Prager, M., Press, W., Alefeld, B. & Huller, A. 1977 *J. chem. Phys.* **67**, 5126–5132.
Press, W. & Prager, M. 1977 *J. chem. Phys.* **67**, 5752–5754.
Ratcliffe, C. I. & Waddington, T. C. 1976 *J. chem. Soc. Faraday Trans.* II **72**, 1821–1839.
Richardson, R. M., Leadbetter, A. J., Bonsor, D. & Kruger, G. J. 1980 *Molec. Phys.* (In the press.)
Rudman, R. & Post, B. 1968 *Molec. Cryst. liq. Cryst.* **5**, 95–110.
Schwartz, R., Post, B. & Frankuchen, I. 1951 *J. Am. chem. Soc.* **73**, 4490–4491.
Stiller, H. 1978 *J. molec. Struct.* **46**, 431–445.
Volino, F., Dianoux, A. J. & Hervet, H. 1976 *J. Phys., Paris* **37**, C355–364.